
Artificial Neural Network-Finite Volume Coupled Model for River Flow

Dr. Kawa Zeidan Abdulrahman, Dr. Jowhar R. Mohammed,

Abstract

This research has been devoted to investigate the capability of using FVM in conjunction with ANNs for hydrodynamic modelling in river flows in order to reduce the computational time required to simulate the impact of an event on hydraulic systems. For this purpose, 2D Godunov-type finite volume model based on unstructured triangular grids was developed. It is second order accurate both in space and time through the use of MUSCL method and a predictor-corrector approach, respectively. The proposed algorithm is tested against two benchmark problems to verify the stability and the accuracy of flow predictions in wetting and drying applications, in the case of existing of bed slope and friction source terms. The ANN-FVM model aimed at reducing the computational time required for numerical simulation of flood flow through reducing the repetitive calculation employing the ANNs ability to generalize beyond the range of training data set. The effects of different activation functions at the hidden layer of MLP neural networks were evaluated for predicting the water levels outside the training data range. Using this model, a noticeable reduction in the repetitive calculations was achieved; as a result, significant reduction in computational time has been gained.

1. Introduction

River floods are complex dynamic processes in which the flow variables have the characteristics of spatial and temporal variations. The hydrodynamic and hydrologic numerical models usually employed for river flood modelling. At the same time, the simulation of river flood using these models often require an expensive computational time. In the recent years, ANNs-based models have been gaining popularity for these applications. The ANN models have the advantage of rapid response: once the ANN models are trained with sufficient data they can be used in their predictive mode to predict the river flow much faster than any numerical model.

The ANN in conjunction with numerical models have been employed to achieve different aims. **Dibike et al. (1998)** investigated the applicability of ANNs for encapsulating a numerical hydraulic model of a river flow and the relative performances of some of the learning algorithms were evaluated. **Dibike et al. (1999)** investigated the possibility of using ANNs as modelling tools for the simulation of tidal flow in a two-dimensional flow field to reduce the time needed to simulate the impact of given input events on hydraulics systems. The results showed that ANNs can be used as a non-linear dynamic systems in capturing the site-specific knowledge. **Tayfur et al. (2005)** developed a finite element model and an artificial neural network model to simulate seepage through Jeziorsko

earth-fill dam in Poland. The results showed that ANN model performed as good as FEM model in predicting the water level in the piezometers, but the ANN required less computational effort.

Based on our knowledge the ANNs in conjunction with the FVM have not been applied to practical river flood. In this research, the possibility of using ANNs in conjunction with FVM to solve the shallow water equations for river flows will be investigated. Simulated flows from a two-dimensional finite volume method are integrated for network training and validation. The ability of the trained networks to extrapolate will be evaluated using flow data beyond the range of the training data sets.

2. The Study Area

The area considered in this study consists of a reach of about 12 km of Diala River (Iraq) begins from downstream of Darbandikhan dam, shown in Fig. (1), and characterized by a complex geometry consisting of narrow bends as depicted in Fig. (2). The maximum depth in the reach was in excess of 21.6 m during peak flood. Diala River is fed by three major tributaries namely, Sirwan, Tanjaro, and Zalm. The topographic data for the study area has been prepared by “landing info worldwide mapping, llc. USA” in the form of Digital Elevation Model (DEM).

Darbandikhan Dam is a rockfill dam with impervious central clay core constructed between 1956 and 1961. The dam has three-bay, gated spillway which terminates in a ski jump and plunge pool with a maximum outflow of $11400 \text{ m}^3/\text{sec}$. The dam is situated in Darbandikhan strait roughly 65 km southeast of Sulaimani (Iraq-Kurdistan Region). The dam is 128 meters high, 535 meters long, and has $3.5 \times 10^9 \text{ m}^3$ storage capacity, and a drainage area of about 17850 km^2 .



Figure (1): Downstream view of Darbandikhan Dam.

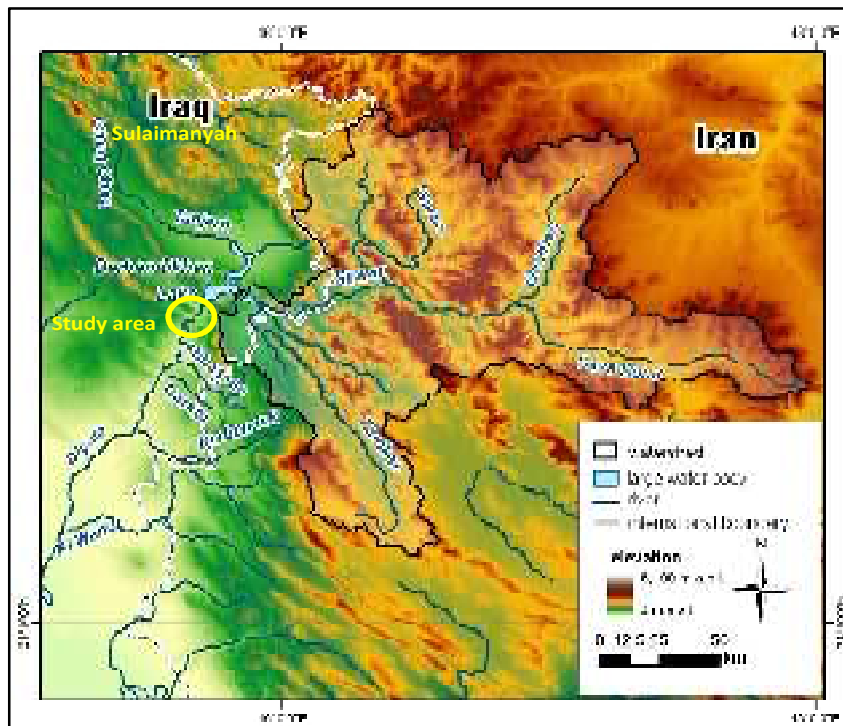


Figure (2): Diyala River and its tributaries adapted from (Irrigation Directorate of Darbandikhan Dam).

3. The Available Data about the Study Area

The river reach under consideration has no data concerning the time series of flow discharge or flow elevation (i.e. there is no gauge station). However, the only available data is a synthetic inflow-outflow hydrograph for the dam reservoir shown in Fig. (3).

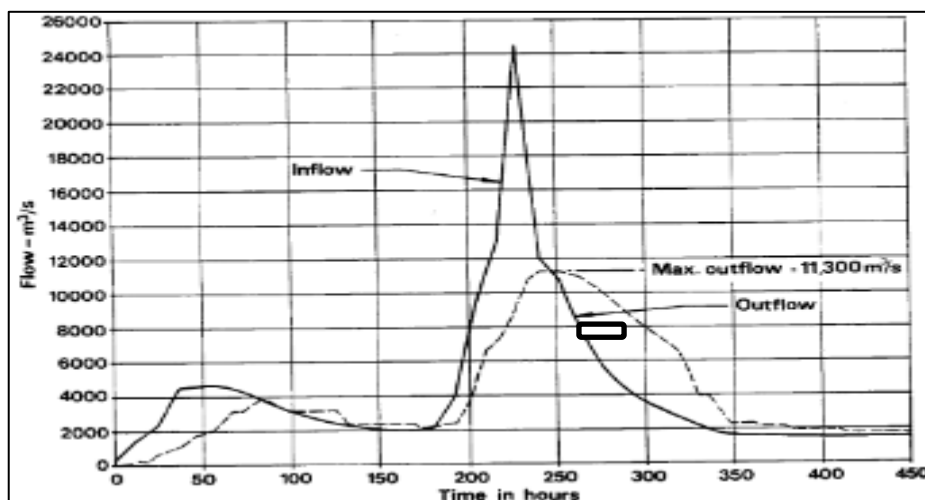


Figure (3): Darbandikhan reservoir inflow-outflow synthetic hydrograph adapted from (Irrigation Directorate of Darbandikhan Dam).

So the outflow hydrograph of the reservoir is converted to discharge time series to be used as inflow boundary condition.

4. Numerical Model

The numerical models presented in this research are based on the Shallow Water Equations (SWEs), i.e., the models perform a numerical integration of the SWEs using a finite-volume approach using unstructured triangular mesh (Yoon and Kang 2004, Anastasiou and Chan 1997, Turan and Wang 2007, Nguyen et al. 2006)..

The continuity and momentum equations are:

$$\frac{\partial U}{\partial t} + \frac{\partial F}{\partial x} + \frac{\partial G}{\partial y} = S \quad (1)$$

where the vector of the conservative flow variables U , the vectors of the mass and momentum fluxes in x and y directions F and G respectively, and the source terms S are defined as

$$U = \begin{pmatrix} h \\ uh \\ vh \end{pmatrix}, \quad F = \begin{pmatrix} uh \\ u^2h + \frac{gh^2}{2} \\ uvh \end{pmatrix}, \quad G = \begin{pmatrix} vh \\ uvh \\ v^2h + \frac{gh^2}{2} \end{pmatrix}$$

and

$$S = \begin{pmatrix} 0 \\ gh(S_{0x} - S_{fx}) \\ gh(S_{0y} - S_{fy}) \end{pmatrix} \quad (2)$$

$$S_{0x} = \tan(\theta_x) = -\frac{\partial z}{\partial x}, \quad S_{0y} = \tan(\theta_y) = -\frac{\partial z}{\partial y} \quad (3)$$

where u and v are vertically averaged velocity components in the x and y directions, respectively; h is the water depth measured from the bed; g is acceleration due to gravity; θ_x and θ_y are the inclinations of the bottom surface in x and y directions. The terms S_{0x} and S_{0y} represent the slopes along x and y direction, and S_{fx} and S_{fy} are defined as friction slopes in x and y directions, respectively. The friction slopes are estimated by using the Manning formula (Zhao et al. 1996, Valiani et al. 2002, Kuiry et al. 2008).

$$S_{fx} = \frac{n^2 u \sqrt{u^2 + v^2}}{h^{4/3}}, \quad S_{fy} = \frac{n^2 v \sqrt{u^2 + v^2}}{h^{4/3}} \quad (4)$$

where n is Manning roughness coefficient.

The unstructured FVM codes used in this study are written in Fortran 90 language (Fortran Power Station Version 4.0). The developed model is able to deal with the wetting-drying conditions for flood plain and wetland studies, dam breaking phenomena, subcritical and supercritical flows, and other practical cases.

5. Neural Network Model

Artificial neural networks (ANN) are powerful solutions to many complex modelling problems. Many studies have demonstrated that the ANN models are very successful in simulating river flows (CIGIZOGLU 2003, Teschl R. and Randeu 2006, Kisi 2005). The highly popular learning rule for multilayer perceptrons namely the back-propagation algorithm (Rumelhart et al. 1986) is used in this research Fig. (4). This algorithm is based on the error-correction learning rule. As such, it may be viewed as a generalization of the delta rule or the least mean square (LMS) algorithm (Haykin 1999). The back-propagation algorithm uses supervised learning. The idea of this algorithm is to reduce the squared error induced due to the differences between the actual and desired outputs. The algorithm is stopped when the value of the error has become sufficiently small.

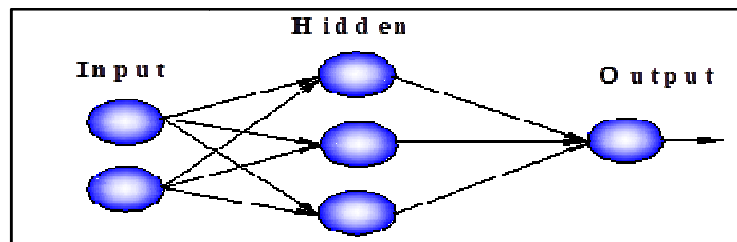


Figure (4): Typical Multi-layer feed-forward network with one hidden layer.

The software chosen to develop the neural networks for this study is the IBM SPSS V.19. ANNs were developed using the neural network tool, which allows a user to specify all the details pertaining to the neural network architecture. These details include the architecture type (e.g. multi-layer perceptron, and radial basis function), the number of hidden layers and processing elements, the transfer functions, and the learning algorithm.

6. Model Verifications

The proposed scheme is tested by comparing the model results with two different benchmark problems, namely the two-dimensional partial dam break problem and the 1D dam break with a triangular hump in the bed.

6.1. Test 1: Partial Dam Break Problem

A partial dam break test is presented to examine the model capability to predict two dimensional flow cases. This model is applied to the 2D frictionless partial dam break with horizontal bed. The computational domain consists of a channel of 200 *m* long by 200 *m* wide bisected by a dam of 10 *m* thickness in the flow

direction. The initial water level is 10 m and 5 m at the upstream and downstream sides, respectively. The water is released through a breach 75 m wide between 95 m and 170 m from one end. The domain is divided into 6456 triangular cells. Figs. (5) and (6) present the contour map and the three-dimensional views of the wave propagation at time 7.2 sec, respectively. There is no analytical solution for this test but very similar plots can be seen in the literatures (Zhao et al 1994, Anastasiou and Chan 1997, Turan and Wang 2007). A very light rise of the water surface at the wave front and a small depression at the middle upstream side can be noticed. These features are also observed in the mentioned literatures.

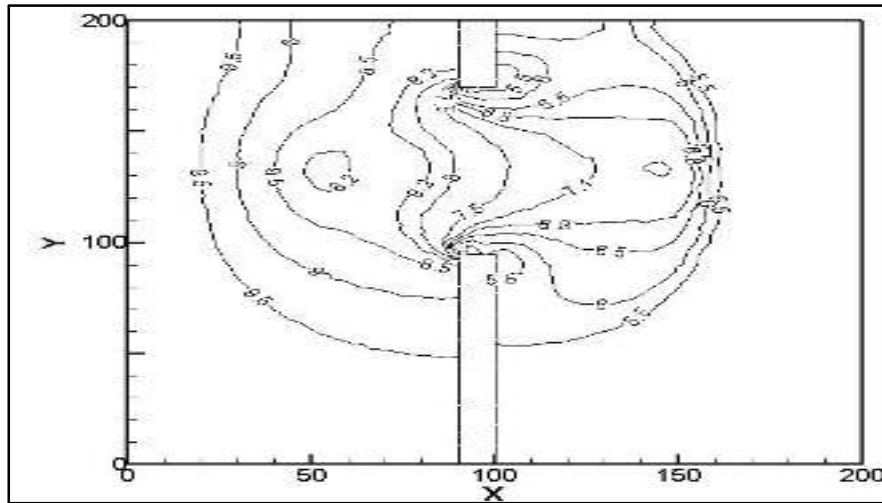


Figure (5): Water depth contour at $t = 7.2 \text{ sec}$ after the dam break.

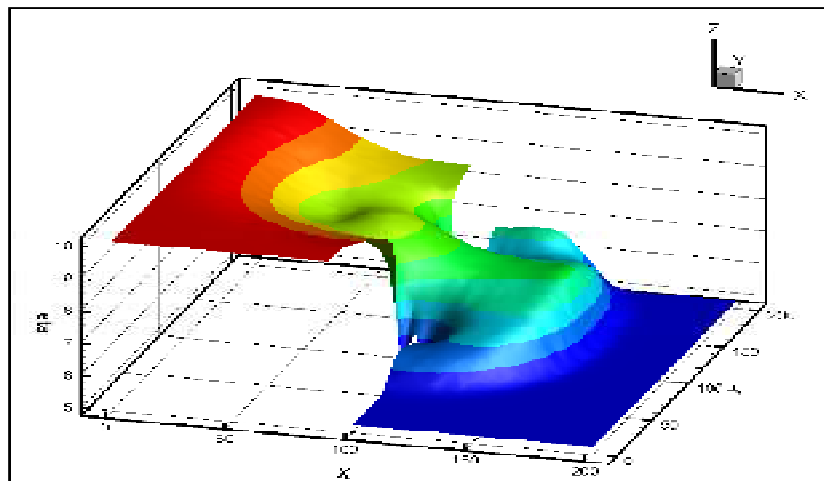


Figure (6): The wave propagation at $t = 7.2 \text{ sec}$ after the dam break.

6.2. Test 2: Dam Break with a Triangular Hump in the Bed

This is an experimental test case carried out by CADAM (the European Concerted Action on Dam-break Modeling) which is an excellent test to check the ability of the algorithm to work on irregular topography with wet and dry beds. It was used by Brufau et al.(2002), and Creaco et al. (2010) considering the dam break flow in a straight channel with a triangular hump of 0.4 m height in the bed to check the numerical model ability to work on irregular topography. The channel has rectangular cross section 38 m long and 0.75 m wide. The dam gate was placed 15.5 m from the upstream end. The initial condition was set such that the depth of the water behind the gate was 0.75 m and the rest of the channel bed was dry as shown Fig. (7). The Manning friction coefficient is $0.0125\text{ sec}/\text{m}^{\frac{1}{3}}$. All boundaries are solid walls except for the free outlet. For the numerical simulation, the domain was divided into 911 triangular cells and the time step was 0.01 sec . The gate was removed instantaneously and a wave propagated over the bed of the channel. Upon reaching the hump, the wave runs up, overtops the hump, and then accelerates down the far side. Figs. (8) and (9) present a comparison between the numerical results obtained using the authors' codes and the experimental data concerning the water depth variations with respect to time at various distances from the gate.

In general, satisfactory fit to the experimental data has been observed for the results obtained from the numerical solution. The scheme is able to capture the sudden rise in the water depth occurring throughout the simulation time due to the shock transit and surge wave.

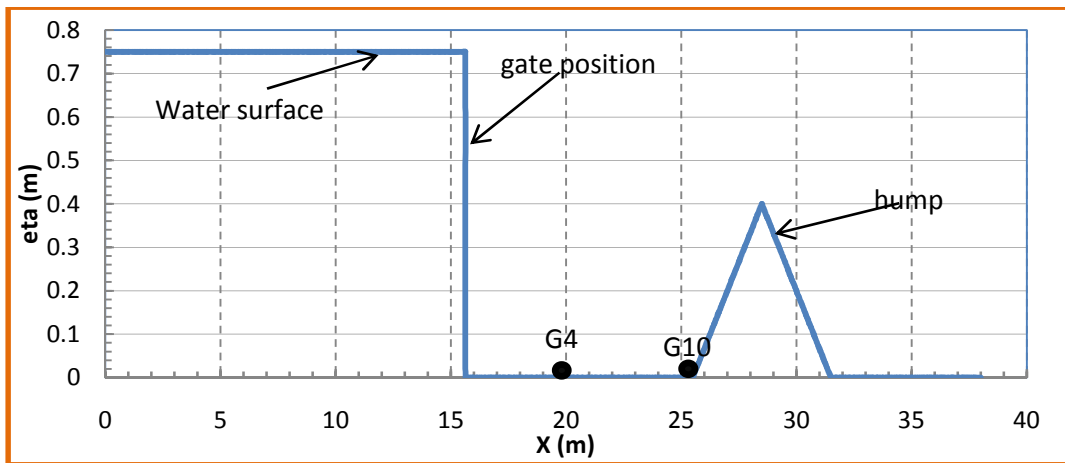


Figure (7): The initial conditions of the dam break test with triangular hump in the bed.

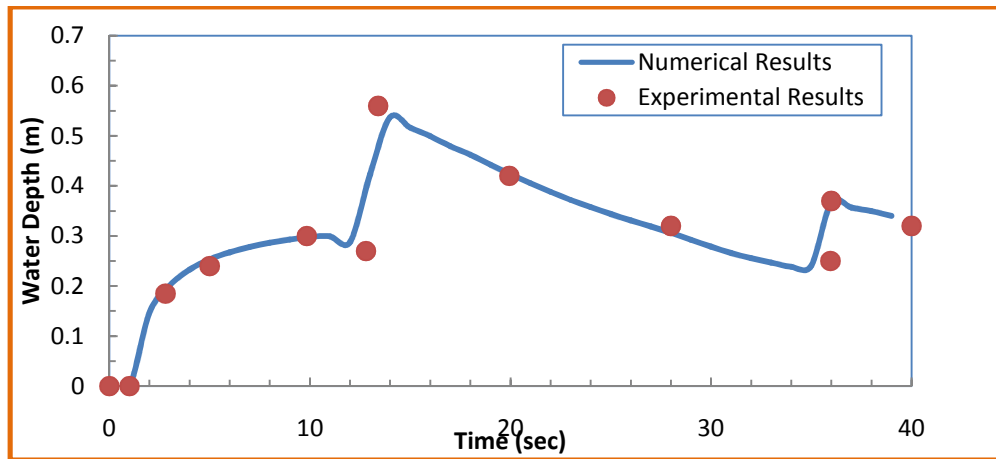


Figure (9): The shock transit at G4.

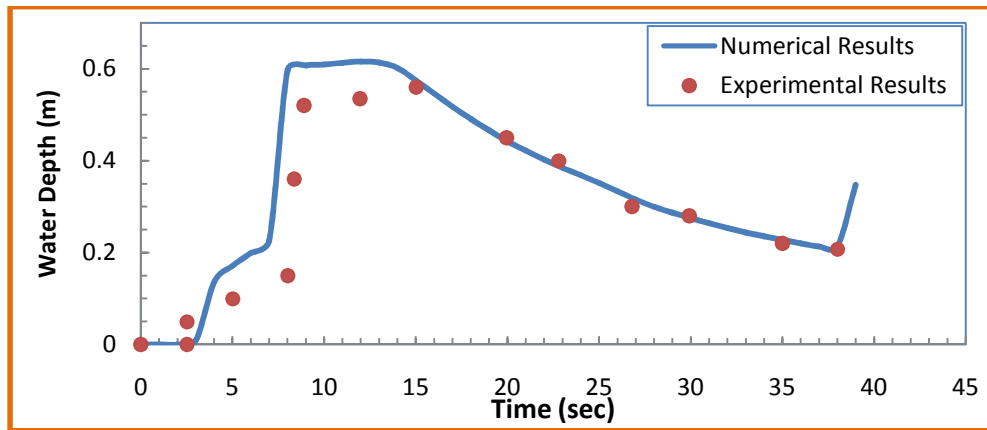


Figure (10): The shock transit at guage10.

7. FVM Simulation (Data Generator)

In order to simulate the flood flow in the river reach, the model area was discretized into 6313 triangular meshes. Local grid refinement was carried out for the lowest area within the river bed which is characterized by relatively narrow cross sections while coarser grids used in the floodplain area as shown in Fig. (11). A constant time step equal to 0.5 sec was used as it resulted in a maximum Courant number lower than 1.0 throughout the simulation period.

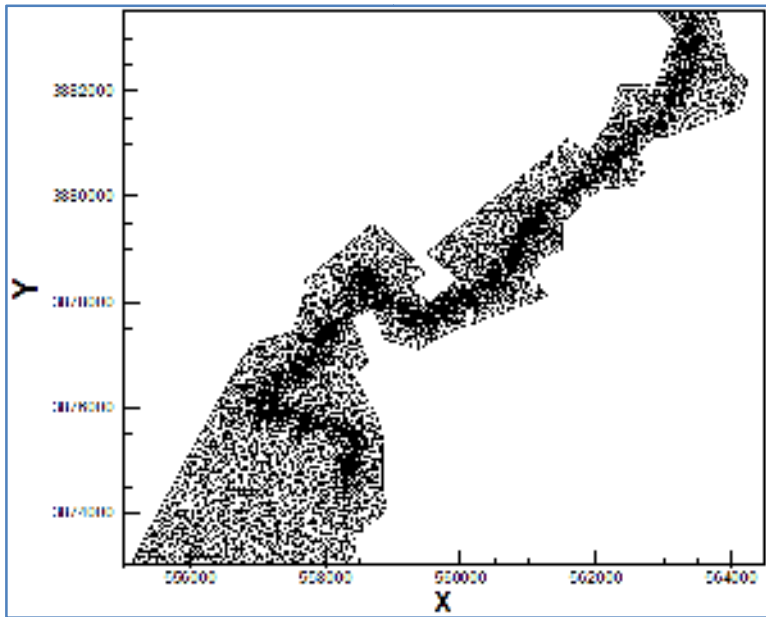


Figure (11): Triangular mesh distribution for the model area.

As it is mentioned earlier, the Darbandikhan reservoir outflow hydrograph would be utilized as inflow boundary for the numerical model. In this context, a portion of the flood hydrograph that is about 160 hours period (approximately 6.7 days) was selected (from time 180 hours to time 340 hours) to be employed for this purpose as indicated in Fig. (12). Moreover, since the downstream boundary condition is not known initially, a non-reflecting downstream boundary condition was used Begnudelli and Sanders (2007). Wall boundary conditions were imposed along the sides of the domain, and the computational domain was broadened in such a way that the full extent of flooding is characterized.

To initialize the model, a small pool of water (with elevation of 378.5 m above sea level) was placed in the river channel next to the upstream boundary and the remainder of the river channel was assumed to be dry as shown in Fig. (13).

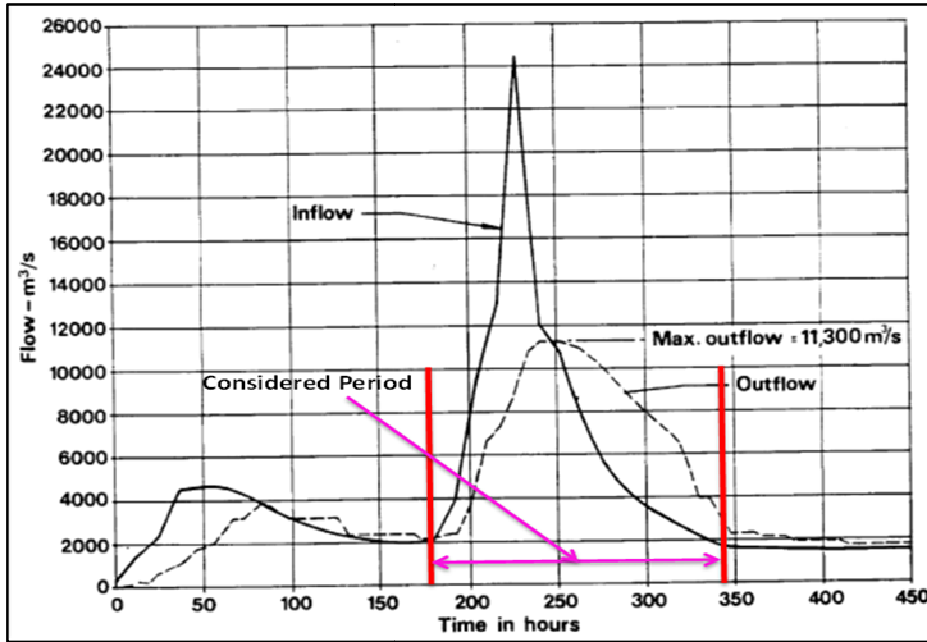


Figure (12): Darbandikhan reservoir inflow-outflow synthetic hydrograph and the selected hydrograph period to be used as input boundary for the numerical model.

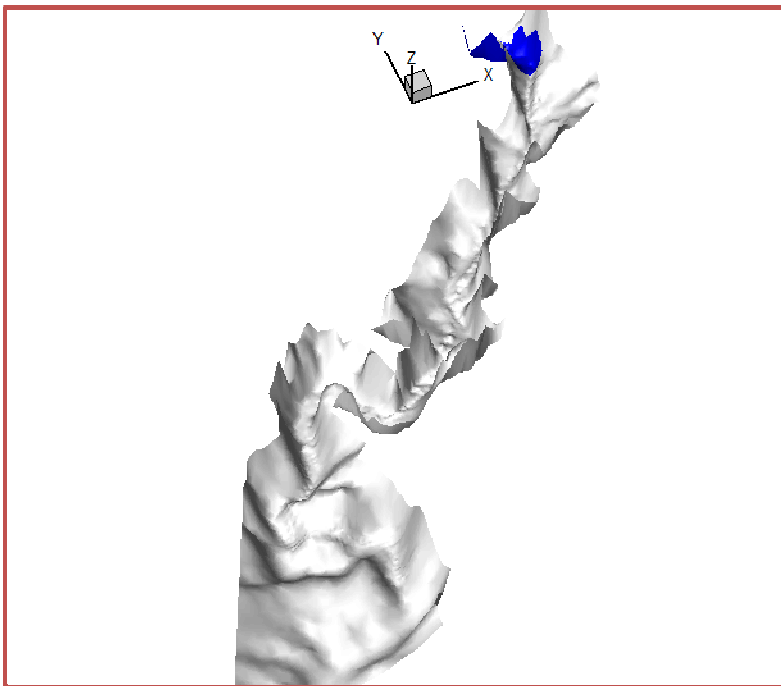


Figure (13): The initial conditions at $t = 0.0sec$ used in the numerical model.

The FVM codes were then run to generate the time series of water levels at each grid point (node) in the model. specified point within the model area was then selected to be modeled by the ANN. Figs. (14) and (15) show the 3D advancement of the flood wave and flooded domain at different times from the beginning of

simulation. In these figures, 3D representation of flooded domains were shown, and may represent an immediate means in order to layout emergency planning, analyzing risk potential and interferences design.

However, the total computation time required for the completion of the entire simulation was approximately 96 hours running on a 1.86 GHz processor Intel Centrino (Toshiba, Satellite).

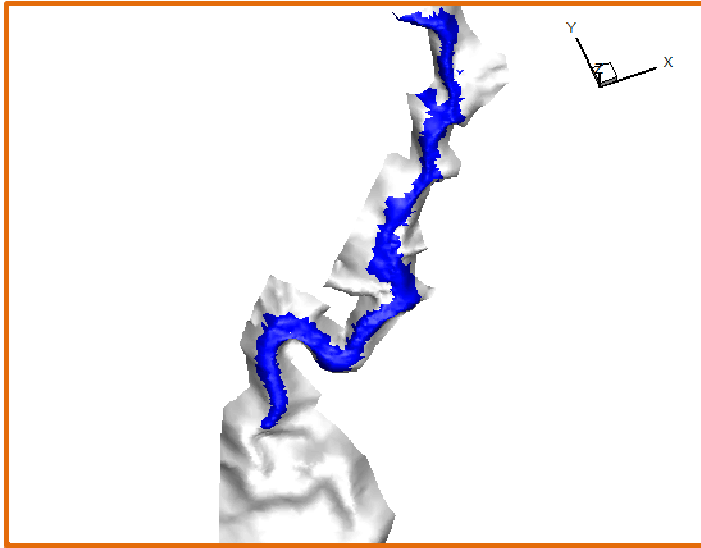


Figure (14): 3D Flood wave advancement at $t = 5760 \text{ sec}$.

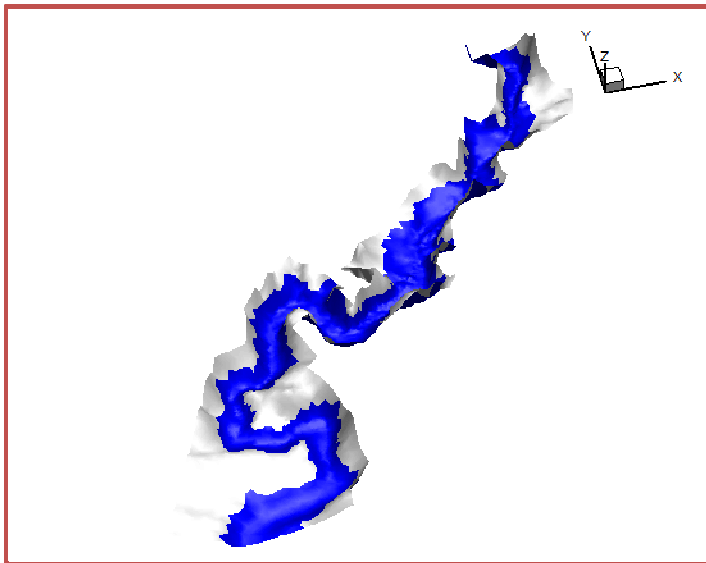


Figure (15): 3D Flood domain at a time corresponding to the largest event.

8. ANN Simulation

The location of point (1) encircled in Fig. (16) to be simulated by the ANN model was identified in the FVM and then the time series of water levels at this point and at the open upstream boundary were prepared.

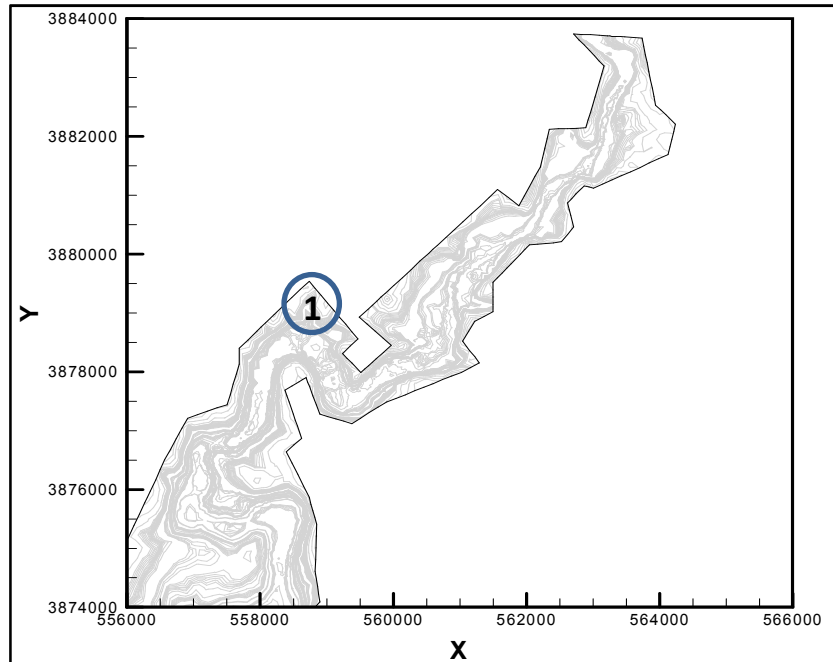


Figure (16): The model area and the point simulated by the ANN.

The data were prepared at 10 *min.* interval and it was divided into training, testing, and validation sets. The data were preprocessed first through excluding approximately the first 4 hours of the flow simulation data to exclude the effect of the initial conditions in the river channel, then the MLP neural networks were used to develop the ANN-FVM model.

9. The Developed Model of FVM-ANN

The numerical models used in simulating river flows usually make a large computational capacity. Practical problem arises, if the river reach becomes further extended and a large scale or high degree of resolution is needed. Computational time increases and makes repetitive calculations very much costly (Chua and Holz 2005). Thus, the question arises as to whether there are other, more economic methods to reduce repetitive calculations.

The present set of experiments aimed at reducing the computational time required for numerical simulation of flood flow by reducing the repetitive calculations in the numerical model. The most evident way to do this with acceptable accuracy is to encapsulate the FVM in ANN form that will enable to extrapolate beyond the training range and allow a much faster simulation. An important criterion in using ANN for flood flow simulation is to predict flows beyond the training data range (Shrestha et al. 2005). ANNs are valuable in these situations, requiring less inputs and computational effort. ANNs can capture the implicit relationship between inputs and outputs, even in highly nonlinear problems (Haykin 1999). ANNs can rapidly produce sensitive responses to small input changes in a dynamic environment.

The input layer neurons of the ANNs for this set of experiments consisted of the time series of water levels at the upstream boundary at different time steps and the time series of water levels at point (1) was specified as the only neuron in the output layer. The whole bounded period of the flood hydrograph depicted in Fig. (12) was used as inflow boundary for the FVM to simulate the time series of water levels at point (1). The numerical results provide the data required for training, testing and validation the ANN models.

In this model, relatively small proportion of the flow variables (water levels) was computed with a sound physically based model (FVM) leaving the major portion to ANN model. In other words, the time series of water levels at point (1) obtained from the numerical simulation running for a part (about 31%) of the flood hydrograph period (bounded in Fig. (17)) was used as training and testing data set for the ANN model. Whereas, the remainder results of the numerical simulation were utilized as validation data set. The maximum flood discharge in the training and testing period was $8500\text{ m}^3/\text{sec}$, while the maximum flood discharge in the validation period was $11300\text{ m}^3/\text{sec}$. Also the maximum water level at point (1) in the training and testing period was 370.4 m and the maximum water level at point (1) in the validation period was 371.9 m .

Methods of improving extrapolation outside the training range were explored. In this context, the neural networks were trained with two different activation functions (hyperbolic tangent and sigmoid) using one and two hidden layers for each one. On the other hand, identity activation function was employed in the output layers. Using identity activation function enables the neural networks to take any range of values (Demuth and Beale 2002). Finally, the trained neural networks were used to simulate the water levels at point (1) for the whole hydrograph period.

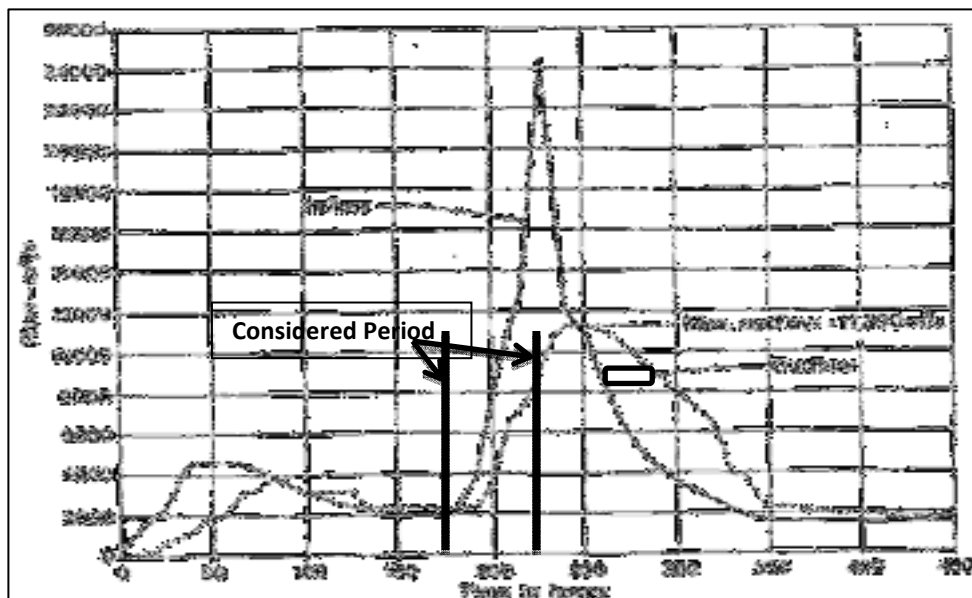


Figure (17): The period of the flood hydrograph used in training of the ANN model.

10. Results

From Figs. (18), (19), (20), and (21), it is apparent that ANN predictions for water levels are to a certain extent close to the FVM prediction. The results revealed that the neural networks can extrapolate to predict river flows beyond the training range with a sufficient degree of accuracy. The performances of different ANN models based on the validation data set in terms of different error measures were summarized in Table (1). In this set of experiments, the Differences in Peak Water Level $DPWL$ obtained from the FVM and the ANN models simulation were considered to evaluate the trained ANN models to extrapolate outside the range of the trained data.

$$DPWL = Eta_{ANN}(max) - Eta_{FVM}(max)(4)$$

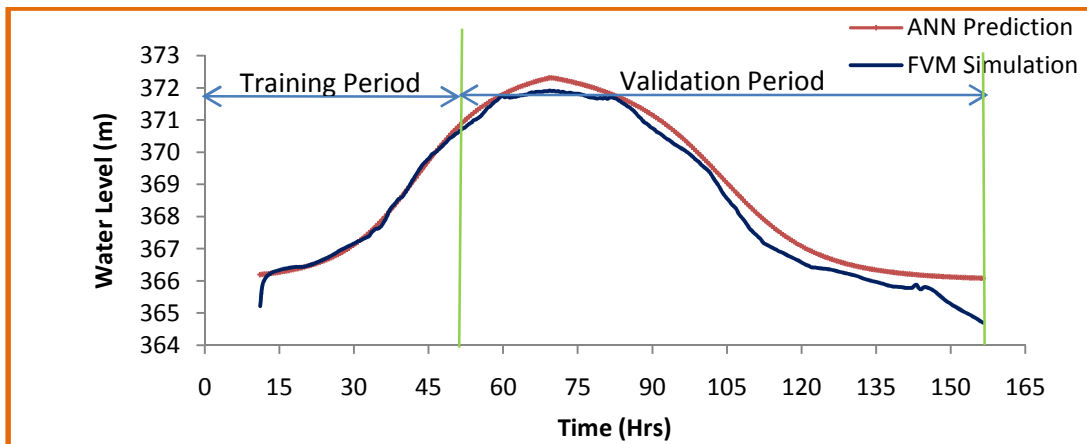


Figure (18): Comparison between water level simulated from FVM and predicted by ANN model using one hidden layer of sigmoid activation function.

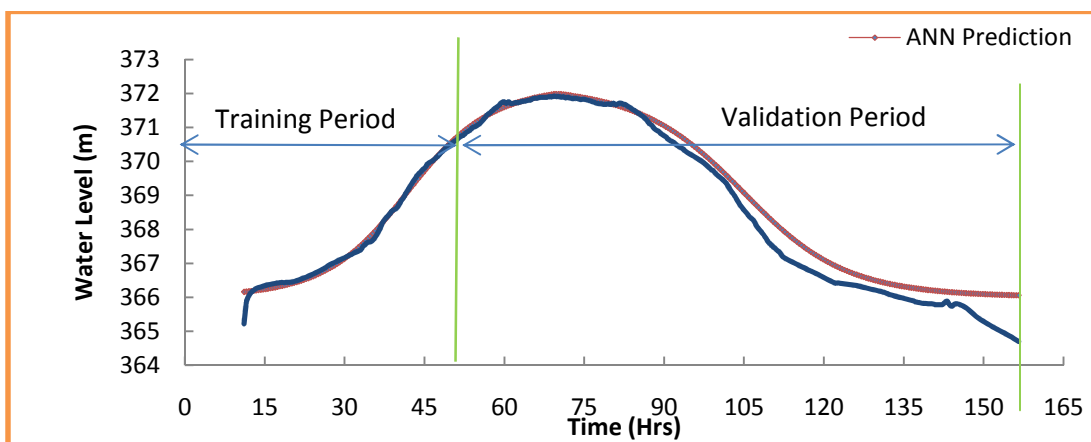


Figure (19): Comparison between water levels simulated from FVM and predicted by ANN model using two hidden layers of Sigmoid activation function.

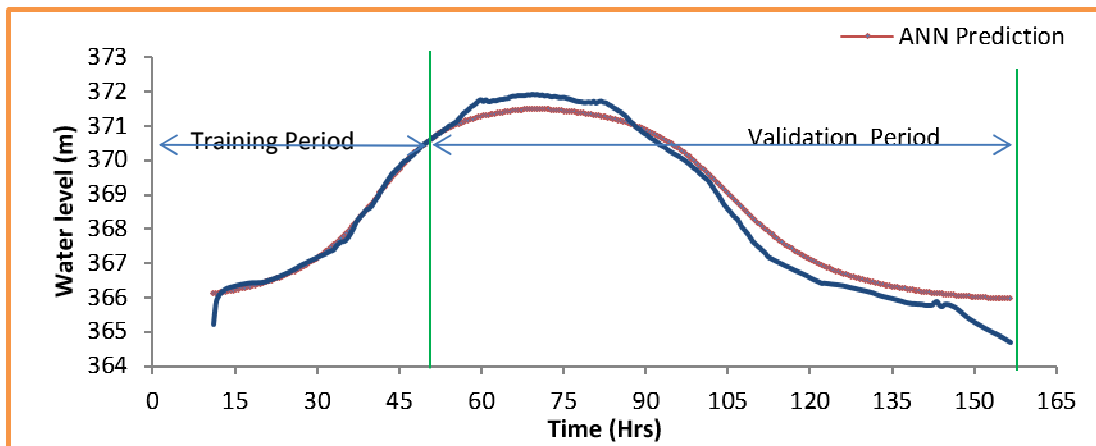


Figure (20): Comparison between water levels simulated from FVM and predicted by ANN model using one hidden layer of hyperbolic tangent activation function.

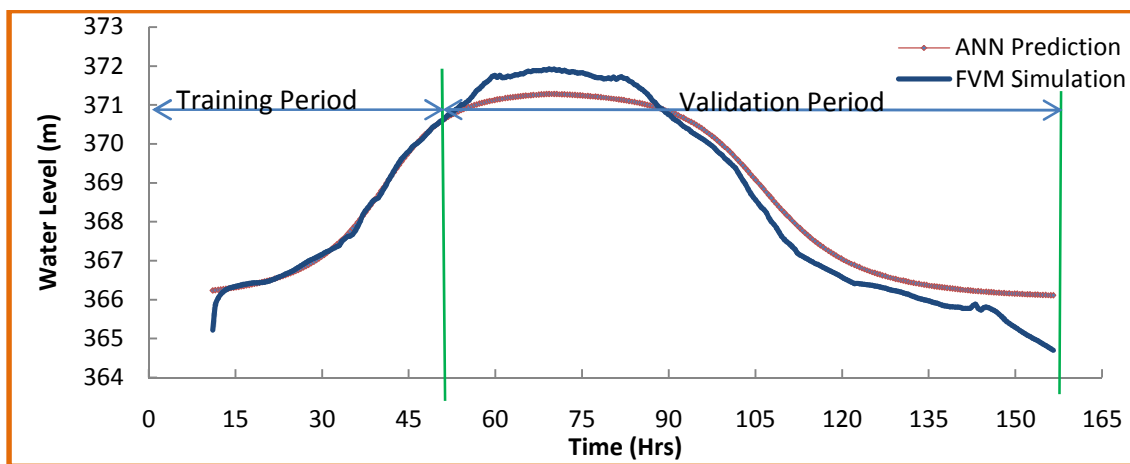


Figure (21): Comparison between the water levels simulated from FVM and that predicted by ANN model using two hidden layers of hyperbolic tangent activation function.

Table (4.5): Performance of different ANN models based on validation data set for prediction of water levels at point (1).

Error	MSRE	CE	MSE	DPWL
ANN Models				
Sigmoid (1 hidden)		0.963		
Sigmoid (2 hidden)	5.49×10^{-5}	0.965	0.201	0.066
Hyperbolic Tangent (1 Hidden)	5.89×10^{-5}	0.957	0.216	-0.412
Hyperbolic Tangent (2 Hidden)	7.71×10^{-5}	0.938	0.286	-0.638

In

general, the ANN models with sigmoid activation function in one or two hidden layers were found to give more

accurate results. Moreover, the ANN models with the hyperbolic tangent activation function had a noticeable tendency to under-predict the peak water level, while the ANN models with the sigmoid activation functions showed a slight tendency to over-predict the peak water level. Although all the used models achieved reasonable accuracy, the best performance in terms of MSRE, CE, and MSE was achieved with the use of the sigmoid activation functions with two hidden layers. The difference in the peak water level was also found to be the least using this configuration. However, all the ANN models showed a tendency to over-predict the recession limb but their over-prediction are not so large to deteriorate the model performance.

The computational time required for simulating the considered part of the rising limb (which used for training the ANN model) and the total period of the hydrograph was 25 and 96 hours, respectively. As a result the saving in the computational time was 71 hours (74% of the total time) for this particular case. Furthermore, for relatively larger models, more computational time will be required since the whole computation will be redone for all elements, nodes, and faces and repetitive calculations will be more expensive. Using this method of coupling between the FVM and the ANN model may be utilized to achieve more economic and time saving model through reducing the repetitive calculations in the numerical simulation of flood flow.

11. Conclusions

Coupling between the FVM and the ANN model is used to reduce the computational time required for numerical simulation of flood flow through reducing the repetitive calculation employing the ANNs ability to generalize beyond the range of training data set. In this context, ANN models were developed through using a part of the data (part of the simulation period) obtained from the numerical model, then, the trained ANN employed to model the total simulation period benefiting from the ANN generalization beyond the training data range. The effects of different activation functions at the hidden layer of MLP neural networks were evaluated for predicting the water levels outside the training data range. Using this model, a noticeable reduction in the repetitive calculations was achieved, as a result significant reduction in computational time has been gained.

Bibliography

12. Anastasiou K., C. T. Chan. (1997). Solution of the 2D shallow water equations using the finite volume method on unstructured triangular meshes. *International Journal for Numerical Methods In Fluids*, 24, 1225-1245.
13. Begnudelli, L., and Sanders, B. F. (2007). Simulation of the St. Francis dam-break flood. *J. Eng. Mech.*, 133(11), 1200-1212.
14. Brufau, p., Vazquez-Cendon, M. E., and Garcia-Navarro, p. (2002). A numerical model for the flooding and drying of irregular domains. *Int. J. Numer. Meth. Fluids*, 39, 247–275.

-
15. Chua, L. H. C., and Holz, K. P. (2005). Hybrid Neural Network-Finite Element River Flow Model. *J. Hydraul. Eng.*, 131(1), 52-59.
 16. CIGIZOGLU, H. K. (2003). Estimation, forecasting and extrapolation of river flows by artificial neural networks. *J. Hydrol. Sci.*, 48(3), 349-360.
 17. Creaco, E., Campisano, A., Khe, A., Modica, C., and Russo, G. (2010). Head reconstruction method to balance flux and source terms in shallow water equations. *J. Eng. Mech.*, 136(4), 517-523.
 18. Demuth, H., and Beale M. (2002). *User's guide of neural network toolbox for use with MATLAB*. (4, Ed.) Natick: The MathWorks, Inc.
 19. Dibike, Y. B., and Abbott, M. B. (1999). Application of artificial neural networks to the simulation of a two dimensional flow. *J. Hydraul. Research*, 37(4), 435-446.
 20. Dibike, Y. B., Solomatine, D. P., and Abbott M. B. (1998). On the encapsulation of numerical-hydraulic models in artificial neural networks. *J. Hydraul. Research*, 37(2), 147-162.
 21. Haykin, S. (1999). *Neural Networks: A Comprehensive Foundation*. Englewood Cliffs, NJ.: 2d ed., Prentice-Hall .
 22. Irrigation Directorate of Darbandikhan Dam. (2010). *Technical report*. Iraq, Darbandikhan.
 23. Kisi, O. (2005). Daily river flow forecasting using artificial neural networks and auto-regressive models. *J. Eng. Env. Sci.*, 9-20.
 24. Kuiry, S. N., K. Pramak, and Sen D. (2008). Finite volume model for shallow water equations with improved treatment of source terms. *J. Hydraul. Eng.*, 134(2), 231-242.
 25. Nguyen, D. K., Shi, Y., Wang, S. Y., and Nguyen, H. . (2006). 2D Shallow-Water Model Using Unstructured Finite-Volumes Methods. *J. Hydraulic Eng.*, 132(3), 258-269.
 26. Rumelhart, D. E., Hinton, G. E., and Williams, R. J. (1986). *Learning internal representations by error propagation*. in: *Parallel Distributed processing, Vol, Foundation1*. Cambridge, MA: MIT Press.
 27. Shrestha, R. R., Theobald S., and Nestmann F. (2005). Simulation of flood flow in a river system using artificial neural networks. *Hydrology and Earth System Science*, 9(4), 313-321.
 28. Tayfur, G., Swiatek, D., Wita, A., and Singh, V. P. (2005). Case study: Finite element method and artificial neural network models for flow through Jeziorsko earthfill dam in Poland. *J. Hydraul. Eng.*, 131(6), 431-440.
 29. Teschl R., and Randeu W. L. (2006). A neural network model for short term river flow prediction. *Nat. Hazards Earth Syst. Sci.*, 6, 629-635.
 30. Turan, B., and Wang, K. H. (2007). Flood and Shock Waves Simulation by using Finite Volume Technique on Unstructured Meshes. [http://dx.doi.org/10.1061/40927\(243\)90](http://dx.doi.org/10.1061/40927(243)90): ASCE.
 31. Valiani, A., Caleffi, V., and Zanni, A. (2002). Case study: Malpasset dam-break simulation using a two-dimensiona finite volume method. *J. hydraul. Eng.*, 128(5), 460-472.

-
32. Yoon, T. H., and Kang, S. K. . (2004). Finite volume model for two-dimensional shallow water flows on unstructured grids. *J. Hydraul. Eng.*, 130(7), 678-687.
 33. Zhao, D. H., Shen, H. W., Tabios G. Q., Lai, J. S., and Tan W. Y. (1994). Finite volume two-dimensional unsteady flow model for river flow. *J. hydraul. Eng*, 120(7), 863-883.
 34. Zhao, D. H., Shen, H. W. , Lai, J. S., and Tabios, G.Q. . (1996). Approximate Riemann Solvers in FVM For 2D Hydraulic Shock Waves Modeling. *Journal of Hydraulic Engineering*, 122(12), 692-701.